ARTICLE

Check for updates

Substantial burial of terrestrial microplastics in the Three Gorges Reservoir, China

Bo Gao [1,4 ✉], Yalan Chen [2,4], Dongyu Xu[1], Ke Sun[2] & Baoshan Xing[3]

Hydropower dams impact the transport of microplastics from rivers to the ocean. The Yangtze River is a large source of plastics to the ocean. Here, we report microplastic concentrations and compositions across a range of size fractions for sediment samples collected in the upper and lower reaches of the Three Gorges Dam in 2008, 2015, 2019 and 2020. We find a gradual increase in microplastic abundance over time, with preferential retention of small-sized (<300 μm) microplastics in the dam reservoir sediments. Small microplastics accounted for between approximately 44 and 90% of identified microplastics, and 82% of all polyethylene particles, which were the dominant polymer type. Our estimate of the total plastic mass load in reservoir sediments suggests that the Three Gorges Dam retains as much as 8048 ± 7494 tons yr^{-1} microplastics in sediments, which is equivalent to 47 ± 44% of the Yangtze River microplastic flux to the ocean.

[1] State Key Laboratory of Simulation and Regulation of Water Cycle in River Basin, China Institute of Water Resources and Hydropower Research, Beijing 100038, China. [2] State Key Laboratory of Water Environment Simulation, School of Environment, Beijing Normal University, Beijing 100875, China. [3] Stockbridge School of Agriculture, University of Massachusetts, Amherst, MA 01003, USA. [4] These authors contributed equally: Bo Gao, Yalan Chen. ✉email: gaobo@iwhr.com

We currently live in the 'plastic epoch' with the ubiquitous presence of microplastics on Earth[1-5]. The marine environment is of particular concern due to its high microplastic contamination[6-8], with the global plastic input into the ocean estimated to be ~10 million tons per year[8,9]. Terrestrial input is the main source of marine microplastics[10], contributing between 64 and 90% of the total plastic input to the oceans[8,11,12]. Extensive dams have been constructed worldwide for hydropower generation, flood control, and shipping, resulting in the fragmentation of free-flowing global river systems[13,14]. Reservoirs that form upstream of the dams decrease flow velocity, increase the hydraulic residence time, trap annually increasing sediment amounts, and subsequently alter the footprints of pollutants[15,16]. The enrichment of microplastics in reservoir surface water close to dams[17] confirms a pressing need to determine the impact of dam construction on the mass-imbalance between plastic debris entering into the ocean and those observed in the ocean[1]. Microplastics burial in sediments is a major plastic sink in marine and terrestrial environments[5,18,19]. Dams are known to exacerbate the accumulation of organic pollutants[20], heavy metals[15], nitrogen, and phosphorus[21]. However, the effect of dams on sedimentary microplastics is largely unknown.

To date, research on microplastic contamination in reservoirs is sparse[19,22-27]. Only 35 out of 183 existing publications about freshwater microplastics reported microplastic contamination in the reservoir region until August 2021[25,26]. Besides, the sizes and polymer categories of microplastics are not well constrained in most previous studies. Substantial uncertainties exist in the assessments of microplastic load by dam interception and an explanation for the global microplastics mass-imbalance is inadequate. This may be due, in part, to the negligence of small-sized microplastics, the small sample sizes, and the lack of close integration between sizes and polymer types. A previous record has reported the preferential accumulation of small-sized microplastics (defined here as <300 μm[28-31]) in riverine sediments[28]. As such, the growing microplastic stocks in reservoir sediments suggest that dams may selectively trap large amounts of small-sized microplastics.

The Yangtze River is the world's third-largest river and the largest input of oceanic microplastics worldwide[10]. The Three Gorges Dam (TGD), located in Yichang along the Yangtze River, is the world's largest hydropower project. The microplastic contamination data of Three Gorges Reservoir (TGR) from the initial operation stage to the stable operation stage is very precious and hasn't been reported yet. Here, we carried out four sampling campaigns in 2008, 2015, 2019 and 2020 to determine the accumulation preference and reorganisation patterns of microplastics during different water-storage stages (Supplementary Fig. 1). During July and August 2020, a catchment-wide flooding with five flood peaks was discharged from the TGD. To investigate the flood-driven microplastic flushing and reorganisation, we compared the microplastic contamination across all sizes and polymer categories in 2019 and 2020[12]. We then estimated the overall mass load of the entire microplastics in the TGR. Based on these results, our study provides new insights into the major role of dams in regulating microplastic fluxes to the ocean. Our data over a 12-year time span is of crucial importance for the microplastic survey.

Results and discussion

Dam promotes deposition of small-sized microplastics in reservoir sediments. In 2020, microplastics were pervasive in all 23 sampling sites, and a total of 2275 microplastic particles were recovered (Supplementary Table 1). The obtained polymers were mainly identified as polyethylene (PE), polypropylene (PP), and cellulose, with minimum diameters ranging from 30 to 3330 μm. The microplastic concentrations at different sites ranged from 1031 to 63,081 items kg^{-1}.

Great spatial heterogeneity was observed in different river reaches within TGR (Fig. 1). Specifically, the lower reach exerted a
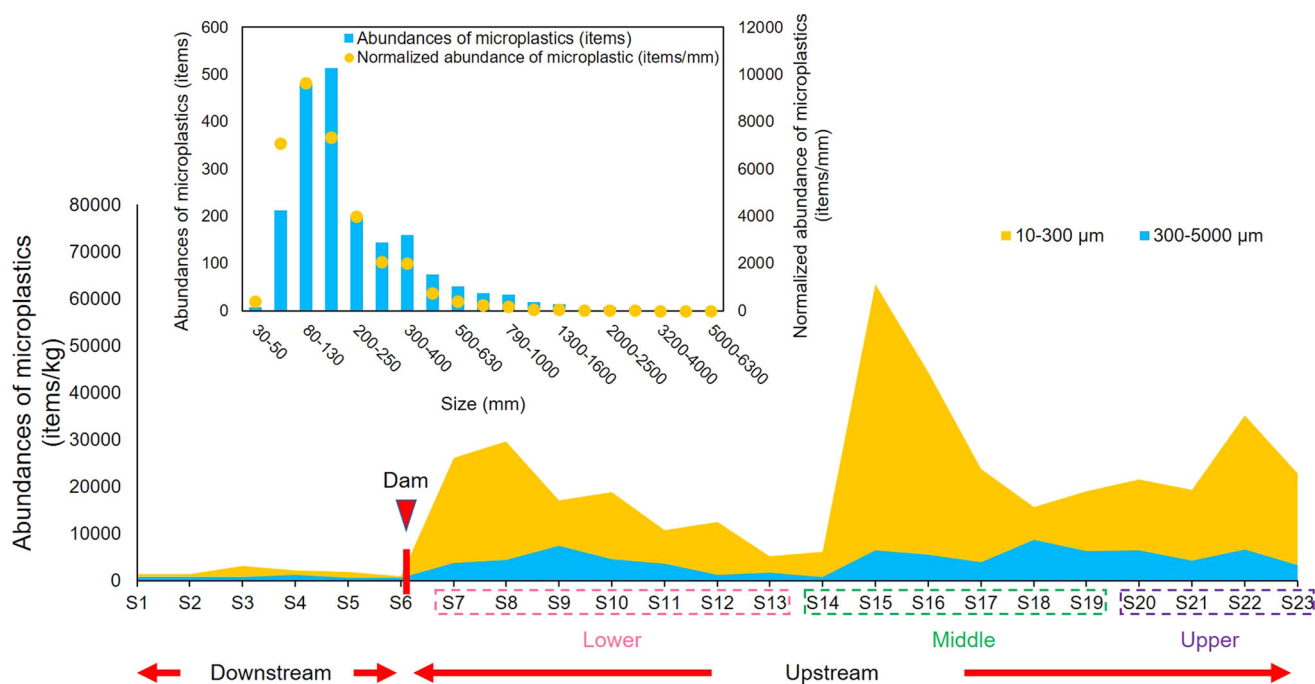
Fig. 1 Size-based abundance of sedimentary microplastics in 23 sampling sites upstream and downstream of the dam in 2020. Microplastic concentrations of the 100–300 and 300–5000 μm fractions are displayed in the main figure. The location of the dam and the division of the upstream and downstream areas, as well as the upper, middle and lower reaches, are marked. The inset shows the size distribution based on the whole identified microplastic particles in the upstream and downstream regions of the TGD in 2020.

much lower microplastic concentration ($17,172 \pm 8604$ items kg^{-1}) than the upper ($24,731 \pm 7128$ items kg^{-1}) and middle ($28,697 \pm 21,052$ items kg^{-1}) reaches of TGR. This can be explained by a variety of factors, including the interference by human activities, the changes in hydrological conditions, the pollution from agricultural activities, and the inflow of upstream microplastics contamination from water, sediments and riparian soils[22,27]. Interestingly, the microplastic concentrations increased with decreasing distance from the dam within the lower reach in TGR (Fig. 1). This is understandable, as the TGD blocks the discharge of microplastics and slows down the water flow in TGR, especially for the sites near the dam. The slowed flow velocity facilitates the deposition of microplastics in the water column close to the dam and the piling up of sedimentary microplastics[5,32].

By comparing microplastic concentrations in sediments collected from upstream and downstream of the dam in 2020, we found that massive microplastics were trapped in the reservoir bed (Fig. 1). The average abundance of microplastics in the sediments upstream of the TGD was $23,018 \pm 14,268$ items kg^{-1} ($n = 1972$), which was more than 12-fold higher than that in the downstream region (1855 ± 765 items kg^{-1}, $n = 303$) ($p < 0.01$). This is consistent with a recent study which reported extensive accumulation of microplastics in the sediment behind dams[16]. Moreover, the small-sized fractions accounted for 75.7% and 55.2% of the total obtained microplastics in the upstream and downstream sediments, respectively. This suggests that the TGR sediments act as a significant intermediate microplastics sink, selectively trapping higher proportions of small-sized fractions. This is understandable, as the dam construction formed a lake-like environment in the reservoir region, which alters the hydrodynamic conditions and thus affects the transport of riverine microplastics into the ocean. The higher microplastic concentration was attributed to the dam entrapment as indicated by the higher microplastic concentration in the surface water in the upstream[17,33], as well as the inflow of non-point source microplastics in the reservoir basin[27]. The dam slows down the flow of water and facilitates the deposition of microplastics into the reservoir bed[5,32]. In addition, the high-calcium and algal-rich environment in the reservoir also facilitates the deposition of microplastics, especially for the small ones[32]. Other processes responsible for the higher concentration of small-sized microplastics in the same sedimentary matrix, including fragmentation and deposition[34], merit further investigations. Irrespective of the small-sized fractions, the remaining microplastic concentrations of the >300 μm size fraction in the upstream were

only 5.7-fold the concentrations of the downstream records. As such, the negligence of small-sized microplastics would result in the gross underestimation of microplastic contamination.

We observed a significant difference in the microplastic size distribution between the upstream and downstream sediments (Supplementary Table 2). The peak size distribution occurred in the 100−300 μm size fraction, followed by the 300−1000, 10−100 and 1000−5000 μm size fractions in the upstream sediments, and the 300−1000, 1000−5000 and 10−100 μm size fractions in the downstream sediments. Among the small-sized fractions, both the 10−100 and 100−300 μm size fractions contributed a higher proportion in the upstream microplastics (17.1 and 58.6%) than the downstream microplastics (5.5 and 49.6%), with higher amounts of the 10−100 μm size fraction selectively trapped behind the dam. Though less abundant in the small-sized fraction, the 10−100 μm size fraction was more inclined to be trapped by the dam than the most predominant 100−300 μm size fraction.

The polymer composition of the small-sized fraction in the reservoir bed varied from that in downstream sediments (Supplementary Table 2). In the order of descending abundance, upstream polymers of <300 μm were mainly comprised of PE (80.5%), PP (12.3%), cellulose (5.2%) and polyethylene terephthalate (PET) (0.5%), while the downstream small-sized microplastics consisted of PE (54.7%), cellulose (21.5%), PP (18.2%) and PET (2.8%). A large amount of small-sized PE was retained in the reservoir bed, while small-sized cellulose, PP and PET were released. As such, small-sized PE played a predominant role in the selective entrapment of small-sized fractions by the dam.

A growing sink of microplastics in the reservoir bed (2008–2020). To further determine whether the reservoir sediments are a major sink for small-sized microplastics, we conducted intensive, systematic, coherent, and repeated investigations on the abundance and distribution of microplastics in the vast and extensive reservoir region during different water-storage stages in 2008, 2015, 2019 and 2020, respectively. Microplastics were detected in all sampling sites, and a total of 8581 microplastic particles were extracted in the upstream of the TGD during the four sampling campaigns (Supplementary Table 1). The microplastic concentration in the reservoir sediment accrued steadily each year (from 3785 ± 3558 items kg^{-1} in 2008 to $23,018 \pm 14,268$ items kg^{-1} in 2020), manifesting the reservoir bed as a growing microplastic sink (Fig. 2a). In addition, the most profound increase
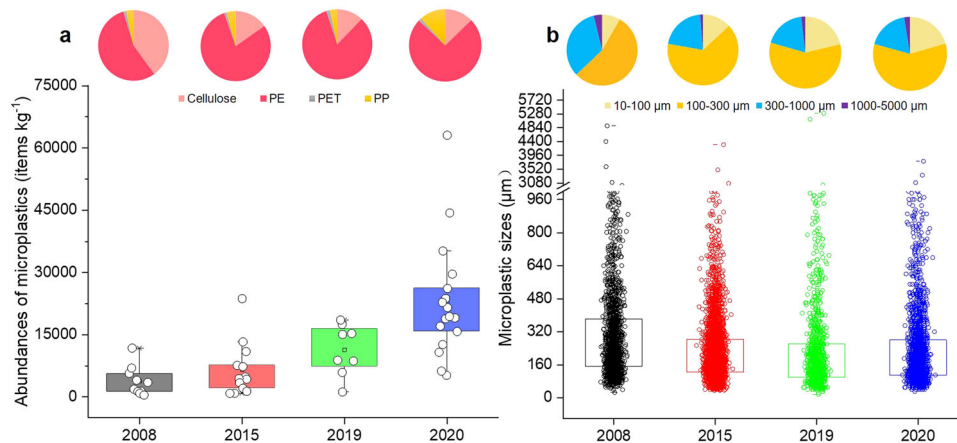
Fig. 2 Interannual variation of microplastics in the bed sediments of the TGR. a Abundance and polymer composition of sedimentary microplastics in 2008, 2015, 2019, and 2020. **b** The size distribution of microplastics in different sampling years. A total of 1804, 3718, 1087, and 1972 particles were identified, examined, and carefully recorded each year (Supplementary Table 1). Boxes show the 25th and 75th percentiles, and error bars represent the 95th percentiles. Black squares and horizontal lines represent the arithmetic means and medians, respectively.

of microplastic abundance from 2019 to 2020 was potentially attributed to the flooding. Previous records have shown that fluvial flooding plays a key role in flushing microplastics from coastal locations and river catchments[12,35–38]. Similarly, flooding would inevitably affect the occurrence and fate of microplastics in the reservoir region. During July and August 2020, a catchment-wide flooding with five flood peaks was discharged from the TGD. Flood no 5 had a peak discharge of 75,000 $m^3 s^{-1}$ on August 17 and was the largest flood since 1981. Instead of efficiently flushing out microplastic particles in the reservoir sediments, the extreme flood greatly enhanced the accumulation of microplastics behind the dam (approximately 1.7-fold higher in 2020 than in 2019, $n = 3059$) (Fig. 2a). The elevated microplastics concentration in one year (from 2019 to 2020: 9843 items kg^{-1}) had even exceeded the decadal increase (from 2008 to 2019: 9390 items kg^{-1}). There are many factors including local lifestyle and economy, waste discharge, flooding, etc. that may contribute to this phenomenon, among which the impact of flooding is non-neglectable. The elevated scouring force and high water level from the flooding event may lead to the flushing of massive amounts of microplastics from both the upper reaches and ambient water-level fluctuation zone into the reservoir bed[12,27,39]. The microplastic enrichment can also be attributed to the enhanced downward transport of microplastics by an intensive hydraulic disturbance in the reservoir bed[5]. Although flood disturbances initially cause an endogenous release of sedimentary microplastics, the dam further blocks the transport of microplastics in the water[17], which intensifies their mixing, sinking, and vertical transport[5].

According to our dataset from 2008 to 2020, the size-related abundance of microplastics in the reservoir bed maintained the descending order of $100-300 > 10-100 > 300-1000 > 1000-5000\,\mu m$ (Fig. 2b). The small-sized fraction was the most predominant and represented 55.1–78.1% of the recovered plastic debris. The predominance of small-sized fractions across different water-storage stages suggests that the burial of microplastics in sediments is a size-selective process. Processes that enhance microplastic density, such as biofilm colonisation[5,40–42], high-density material bonding (e.g. suspended sediments[43], natural organic matter[44] and extracellular polymeric substances[45]), and aggregate formation[46], are more prone to occur on smaller particles with higher specific surface areas[47–49], and appear to be one explanation for the preferential accumulation of small-sized microplastics in sediments. Compared to the marine environment, such processes may be more prevalent in freshwater systems due to the lower water density of ~1 $g\cdot cm^{-3}$, which promotes the settling of microplastics from the water column[50]. Moreover, the decreased flow velocity and enhanced hydraulic retention time in reservoirs can enhance the homogeneous and heterogeneous aggregation of microplastics and facilitate their vertical transport[5,32], especially for smaller microplastics[48,51–53]. After sinking, these small-sized microplastic aggregates may remain negatively buoyant and hidden beneath the surface water[49], while larger plastic debris are at higher risks of breaking down into smaller pieces and regaining buoyancy to migrate upwards due to the non-uniformity of fouling[54]. As such, our understanding of the trigger mechanism of particle size on the downward transport of microplastics is far from robust and requires further investigation.

During the experimental impoundment stage in 2008 (operating at a high water level of 172.89 m for the first time), reservoir sediments contained a higher proportion of the >300 μm size fraction than sediments in 2015−2020 (Fig. 2b). We attributed this apparent mismatch in the size distribution in 2008 to the remaining litter along the water-level fluctuation zone caused by population migration. During the stable operating stage after 2010, the different water-storage stages had not yet significantly

modified the size distribution of microplastics. Notably, we observed no significant changes in their size distribution, even after the massive flooding event, which is also supported by the minimally altered size distribution by catchment-wide flooding in northwest England[12]. Our long-term assessment of microplastic contamination over a spatially extensive transect in the TGR highlighted the continuously predominant occurrence of small-sized microplastics.

PE dominates the undervalued small-sized microplastics in reservoir beds. A total of 10 polymer types (PE, cellulose, PP, PET, polyvinyl chloride, polyamide, polystyrene, polyacrylamide, polyurethane and polyvinyl alcohol) were identified in sediments by μ-FTIR (Supplementary Fig. 2). In the order of descending abundance, the dominant polymer types, PE, cellulose, and PP, accounted for more than 84% (84.4–97.9%) of the recovered microplastics (Fig. 2a). PE was the most abundant and ubiquitous polymer group, ranging from 54.5 to 82.0% during 2008−2020. The dominance of PE is partly because it is one of the most produced and discarded plastics globally. Our findings are consistent with previous observations, in which PE dominated the polymer compositions in sediment[55,56], Arctic ice cores[2], and the Atlantic Ocean interior[1]. Interestingly, PE is of lower density than other polymers as well as freshwater, but it could finally end up in reservoir sediments. One explanation is that PE is mainly comprised of small-sized particles[56], and its density can be more readily altered by biofouling[5,40–42], incorporation into microalgae aggregates[45], and encapsulation within faecal pellets[46]. Moreover, the dam slows down the flow of water and facilitates the deposition of microplastics into the reservoir bed. The high-calcium and algal-rich environment in the reservoir region further facilitates the deposition of PE[45].

The obtained polymers in 2008 were comprised of 54.5% PE, 39.4% cellulose and 3.3% PP, which significantly differed from the composition in subsequent sampling records (Fig. 2a). As previously mentioned, the undisposed plastic litter from population migration may explain this discrepancy. In 2015 and 2019 during the normal dam operation stage, the microplastics consisted of 78.7–82.0% PE, 12.1−15.0% cellulose, and 3.4−4.1% PP, and their contributions barely changed during the 4 years. Even in 2020 after the flooding, the polymer composition distribution only changed slightly, with PP increasing from 3.4 to 9.9% and PE decreasing from 82.0 to 63.4%. As such, the polymer composition in reservoir sediments has not been significantly modified by varied hydraulic conditions or even massive flooding[12], and appears to be mainly associated with the surrounding economic/social development and living characteristics along the upstream of the Yangtze River. However, we did not observe clear evidence for the fixed use patterns of plastic types or proportion in target areas; therefore, the associated regional plastic consumption requires further research.

The size of all the recovered polymer groups ranged from 16 to 5000 μm (Supplementary Table 1). Approximately 81.6% of PE, 5.9% of PP, 10.8% of cellulose and 0.4% of PET were <300 μm (Fig. 3a and Supplementary Fig. 3). This suggests that previous negligence of small-sized microplastic measurements has led to gross underestimations in the abundance of most littered PE. With respect to the small-sized fractions, PE (68.4–91.2%) had a higher contribution compared to cellulose (4.3−24.9%) and PP (3.0−12.3%) (Fig. 3b). The predominance of PE in small-sized fractions at all our sampled locations during different years suggests that the size-selective entrapment by the dam was closely associated with polymer type. This is understandable, as different polymers possess diverse surficial properties (e.g. hydrophobicity and surface topography)[57] and exhibit varied binding abilities
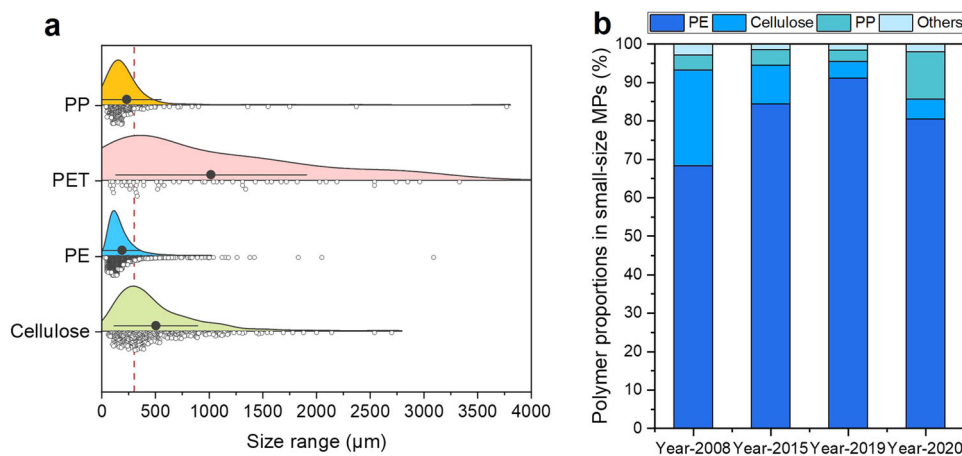
Fig. 3 Polymer-specific size distribution of sedimentary microplastics. Proportion of different size microplastic groups in the four dominant polymer types, including cellulose, PE, PET, and PP (**a**). Polymer composition in the small-sized microplastics in different sampling years (**b**). The size distribution of different polymers was concluded based on the statistical results of 8581 counted microplastic particles. The black hollow circles represent the data points that make up the size distribution of microplastic particles. The black solid circles refer to the mean particle sizes and the horizontal bars indicate the ±standard deviation.

with biological and abiotic materials[42,43]. Moreover, different polymers and their adsorbed organic matter may provide varied carbon sources (e.g. the recalcitrant C of the plastic itself[58,59] and the unstable C, such as plastic-derived dissolved organic matter by initial photodegradation and adsorbed additives[59–61]), and their corresponding biofilm growth can differ. For example, biofilm formed on the surface of different microplastics had distinctive features and led to various density changes in microplastics[42]. Thus, the negligence of small-sized microplastics introduces serious uncertainties in the estimations of both overall and polymer-specific abundance and risks. Due to the small sample size, previous studies have rarely conducted integrated analyses of polymer types and particle sizes[28]. The polymer compositions of most previous records were limited to the >300 μm microplastics (Supplementary Table 3) and are therefore not directly comparable with our study. Therefore, investigations based on large sample sizes across all sizes and polymer categories are necessary to more accurately assess the size-based and polymer-specific microplastic contamination.

Estimated load of microplastics in reservoir sediments. According to the *Yangtze River Sediment Bulletin*, sediment deposition in the TGR was 185.6, 27.8, 59.1 and 144.3 million tons in 2008, 2015, 2019 and 2020, respectively[62]. The corresponding average microplastic concentrations were 3785, 6422, 13,175 and 23,018 items kg^{-1}, respectively. By multiplying the microplastic concentration with the annual sediment deposition, the quantity load was estimated to be 1245 ± 1410 trillion particles per year, with small-sized microplastics accounting for 932 ± 1084 trillion particles per year (Table 1). Hence, dams will significantly modify the footprints of riverine microplastics, which helps to refresh the overall picture of global microplastic contamination. Here, we only use the total amount of sediment deposition for calculation, since our aim is to obtain the magnitude order of microplastic contamination data. Another reason is that it's scarcely possible to measure the sediment deposition rate to obtain a very accurate amount of siltation, since TGR is the world's largest reservoir with a catchment area of 1084 km^2 and a water depth of 100 m.

The annual mass load of microplastics was estimated to be 8048 ± 7494 (529 − 17,822) tons year^{-1} (Table 1), which is equivalent to 0.0025 ± 0.0022% of the global annual plastic production (245, 322, 368 million tons in 2008, 2015 and 2019, respectively)[63] and 47.3 ± 44.1% of the largest annual plastic outflow worldwide (17,000 tons year^{-1} in Yangtze River)[10]. However, our estimation of microplastic burial in the reservoir bed is higher than the annual plastic outflow in the Yangtze River based on an in-situ measurement by ref. [34]. As one can readily see remarkable amounts of microplastics are trapped by a single dam.

The microplastic mass loads in different years in the TGR differ markedly (Table 1). This can be attributed, in part, to the large temporal heterogeneity of the average particle mass. The average particle mass in the bed sediments of the TGR was calculated as 13.60, 2.96, 5.50, and 5.37 μg item^{-1} in 2008, 2015, 2019, and 2020, which had consistent order of magnitude with a previous estimation based on in-situ measurement[34]. As such, large uncertainties exist in the estimations of microplastic mass burdens[64], and extensive measurements of average particle masses of global microplastics are needed. Despite the diversity in the average particle masses of all-sized microplastics, the average particle mass of small-sized fractions was similar (0.41, 0.49, 0.44 and 0.43 μg item^{-1} in 2008, 2015, 2019 and 2020). The corresponding mass proportion of small-sized microplastics were 1.9, 13.0, 6.3 and 6.1 wt% (equivalent to 181.61, 68.58, 234.57 and 1082 tons annually), respectively. Although the quantity load of small-sized microplastics in the reservoir bed is extremely high, the mass burden is relatively low.

Comparison with global-scale freshwater sediments. By mining and ranking the comparable datasets of microplastic contamination in worldwide freshwater sediments, we found that microplastic abundance in the TGR (23,018 ± 14,268 items kg^{-1}) in 2020 was profoundly higher than that in most studies (0.5−3315 items kg^{-1}) (Fig. 4 and Supplementary Table 3), including the riverine and marine sediments, as well as the reservoir sediments[56,65,66]. This was attributed, in part, to the negligence of small-sized microplastics in most of the previous observations. Exceptionally, ref. [28] reported comparable but higher microplastic concentrations (32,947 items kg^{-1}) in the sediments of the Wen-Rui Tang River (in China) than in this study, as they also considered small-sized microplastics.

A direct comparison of size distribution among different studies is challenging due to the different sampling, analytical, and size-division approaches applied in different studies

Table 1 Average particle mass, quantity load and a mass load of entire and small-sized microplastics (SMPs).

| Sampling year	Abundance (items kg^{-1})	Quantity proportion of SMPs	Average particle mass (μg item^{-1})		Quantity load (trillion items)		Mass load (tons)		Mass proportion of SMPs
			MPs	SMPs	MPs	SMPs	MPs	SMPs	
2008	3785	62.9%	13.60	0.41	702	442	9554	182	1.9%
2015	6422	77.8%	2.96	0.49	179	139	529	69	13.0%
2019	13,175	79.3%	5.50	0.44	779	617	4286	272	6.3%
2020	23,018	76.2%	5.37	0.43	3321	2531	17,822	1082	6.1%

(Supplementary Table 3). Small-sized microplastics accounted for 75.7% (44.4−89.7.0%, $n = 1972$) of our recovered plastic debris in sediments in 2020, while common sampling techniques in previous investigations potentially ignored this huge proportion by using a >300 μm sieve[67,68]. Thus, all-sized investigations are essential to eliminate the uncertainty in microplastic contamination measurements.

Dams fragment the transport patterns of riverine microplastics into the ocean and significantly impact terrestrial ecosystems. Our results demonstrate that a remarkable amount of terrestrial microplastics is not exported to the ocean due to dam entrapment, underscoring the importance of accounting for dams when investigating global riverine microplastic transport. According to the *International Commission on Large Dams*, more than 58,000 large dams (defined as those with a height of >15 m or between 5−15 m and impounding more than 3 m^3) are currently in operation, which fragment the free flow of global rivers[69]. Thus, the focus should be placed on the microplastic burdens of global-scale reservoirs. Moreover, dam constructions alleviate the oceanic burden of microplastics and provide a potential opportunity for future oceanic plastic remediation. Also, the transformation of reservoir dispatching methods could enhance the possibility of regulating the flux of microplastics to the sea. Our data also revealed the selective entrapment phenomenon of small-sized microplastics in the reservoir bed. The significance of investigating microplastic contamination across all sizes and polymer categories has been suggested previously[1,8]. Our observations further stress the importance of integrated analyses of polymer types and particle sizes based on large sample sizes. With respect to smaller microplastics of <10 μm or even <1 μm, significant knowledge gaps on their abundance, fate, and risks highlight the need for critical investigations in the future.

Methods

Study area. This study focused on two areas around the TGD: the reservoir region (upstream of the dam, covering a catchment area of 1084 km^2) and the downstream area of the TGD. The operation of TGD, the world's largest hydropower project, has brought about significant benefits for hydropower generation, flood control and shipping[70]. The total length of the dam axis is 2309.47 m, the crest elevation is 185 m, and the designed water level is 175 m. The total storage capacity is 39.3 billion m^3, including 22.15 billion m^3 for flood control. The TGD is located in the Yangtze River—the world's third-largest river. The Yangtze River Economic Belt is densely populated with intensified economic activities; it is also the highest emitter of oceanic microplastics worldwide[10]. To regulate fluvial flooding, the TGR region exhibits anti-seasonal water fluctuation, which inevitably regulates the footprints of riverine microplastics along the catchment. The sediment budget is an important factor affecting the life cycle of a reservoir. In recent years, the sediment burden in the TGR has been efficiently alleviated due to its operating mode of storing clear water and discharging muddy water (Text S1)[71]. The construction of upstream cascade reservoirs is another important factor controlling the TGR sediment budget[72].

Experimental design and bed sediment sampling. In this study, four sampling campaigns were conducted in 2008, 2015, 2019 and 2020 to determine the inter-annual variation of microplastic contamination in the reservoir bed. The first batch of sediment samples were collected in 2008 during the first experimental high water level of the TGR at 172.89 m. During this time, large amounts of litter generated by population migration were casually discarded in the reservoir area. Moreover, the hydro-fluctuation belt of the reservoir had not been completely formed. This batch of sediment samples, therefore, reflected the initial microplastic contamination in the TGR. The second batch experiment was conducted in 2015, during which a stable high water level of 175 m (the designed maximum water level) was maintained since 2010. The third batch was conducted in 2019 before the massive flooding in 2020. We then resampled the sediments in the reservoir bed in 2020 to investigate the driving effects of flooding on microplastic reorganisation. Moreover, the sediments downstream of the TGD in 2020 were also sampled to evaluate the retention effects of the dam. During July and August 2020, an extraordinary and intensified flooding event with five flood peaks affected the upstream of the Yangtze River. Flood no 1 peaked at 53,000 m^3 s^{-1} on July 2; Flood no 2 peaked at 61,000 m^3 s^{-1} on July 17; Flood no 3 peaked at 60,000 m^3 s^{-1} on July 26; Flood no
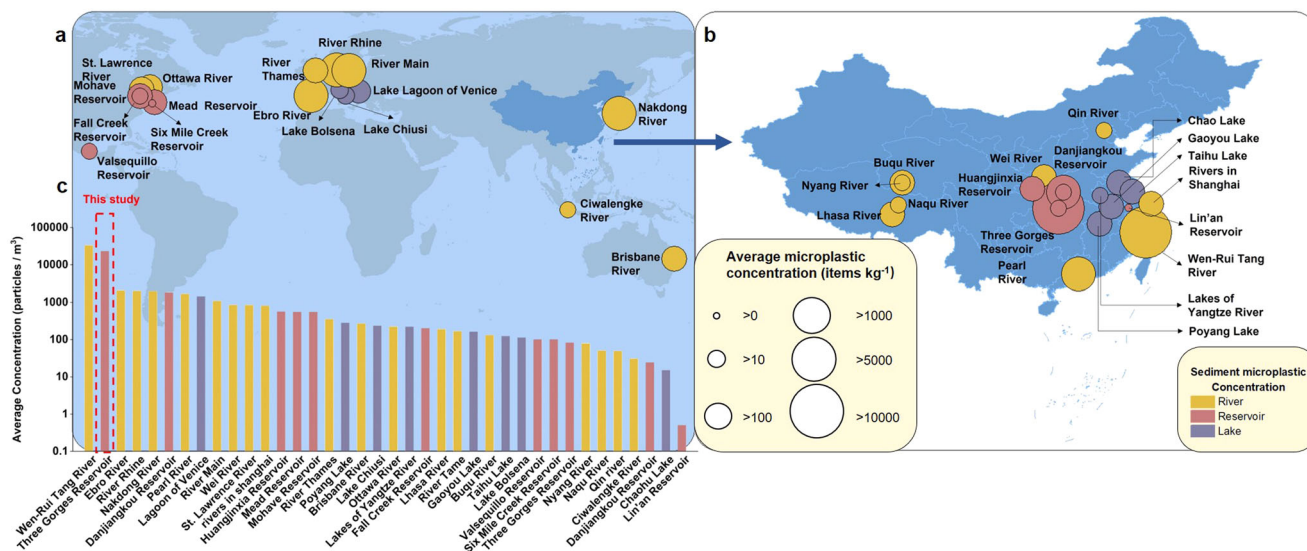
Fig. 4 Global microplastic abundance in freshwater sediments. Sedimentary microplastic concentrations are mapped as the average concentration on the global scale (**a**). Microplastic concentrations in the inset blue region (China) are mapped in higher detail (**b**). A total of 37 comparable records with consistent units are mined and ranked (**c**). The size of the circles represents the average microplastic concentration. The colours of the circles and bars represent River, Reservoir, and Lake. The axis of ordinates shows the average microplastic concentration by an exponential gradient. Detailed information on the sampling sites, polymer compositions, and particle sizes in the literature is provided in Supplementary Table 3.

4 peaked at 59,000 m^3 s^{-1} on August 15; Flood no 5 peaking at 75,000 m^3 s^{-1} on August 17, exceeding the second largest flood peak of 63,300 m^3 s^{-1} in 1998.

During the four designed sampling campaigns covering different water-storage stages, we sampled the top 20 cm of the bed sediment matrix and collected 56-bed sediment samples. A total of 12 common sampling sites near the hydrometric station were designed every year. The sampling sites almost evenly covered different river reaches in the reservoir area. However, a few sampling sites were inaccessible for several years due to the water level or velocity variation, resulting in the failure to obtain sediment samples in certain sampling sites. In order to investigate the effects of the dam on the microplastic composition in the upstream and downstream of TGD, as well as in the upper, middle, and lower reaches within the TGR, we supplemented five sampling sites on the basis of 12 sampling sites in the upstream region, and set up another six sampling sites in the downstream region in 2020 (Supplementary Fig. 1). The supplementary five sampling sites barely altered the overall microplastic contamination status in the upstream region. All the sampling sites were located near the hydrometric station and evenly covered different reaches along the mainstream. In 2020, there were 4, 6 and 7 sampling sites in the upper (S20–S23), middle (S14–S19) and lower (S7–S13) reaches of TGR, respectively.

Bed sediments were collected using stainless steel grabs and retrieved manually or with the help of a winch. At each sampling site, ~1 L of sediment (0−20 cm) was collected with a Van Veen grab and placed in an aluminium foil bag. Three replicates were taken randomly at each site and mixed homogeneously to form one composite sample. The fresh samples in the aluminium foil bag were then immediately transported to the laboratory. The sediment samples were thoroughly mixed, air-dried, and stored in a dark and cool place.

Microplastic extraction and identification. Before microplastics extraction, ultrapure water was added to 50 g of dried sediment samples. Then, the mixed sample was passed through a 5-mm sieve. The sediment fractions of <5 mm were used to extract the microplastics based on the National Oceanic and Atmospheric Administration (NOAA) protocol with minor modification[73]. The zinc chloride (ZnCl$_2$) solution ($\rho = 1.6$ g cm^{-3}) was filtered through a 0.45 μm cellulose acetate membrane (Milli-Q, 47 mm diameter, U.S) to remove the impurities in the reagent. The two-step density separation was used in this study. Approximate 200 mL of ZnCl$_2$ solution was added to 50 g dry weight of sediment samples in a glass beaker (250 mL), stirred with a glass rod for 2 min and settled for 24 h. The suspension of the aqueous solution was filtered via vacuum filtration through the stainless steel sieve (10 μm). The floating particles on the sieves were washed with the ultrapure water into a beaker and subsequently covered with aluminium foil paper. The process was repeated sequentially three times, and the supernatants were combined. After the density flotation, the solution was treated with a 20 mL Fenton reagent (acidified 0.05 M FeSO$_4$) and 20 mL of 30% hydrogen peroxide solution to remove the organic materials in the supernatant[74]. Following organic removal, the supernatant of the aqueous solution was filtered through silver filter paper (Milli-Q, 0.45 μm, 25 mm diameter, U.S). The filter papers were transferred to the glass Petri dishes and dried at 50 °C for further identification.

Suspected microplastics on the filter membrane were picked up onto the barium fluoride window (13 mm diameter, Thermo Scientific, USA), and were photographed under a stereo microscope (SC-III, Shanghai, China) to record the colour, sizes, and morphological types (i.e. fragment, film and fibre). Then, this barium fluoride window was placed in the micro-Fourier transform infrared spectrometer (μ-FTIR, Nicolet iN10MX, USA). The transmission mode was used to identify the spectrum of suspected particles with wave numbers from 650 to 4000 cm^{-1}. The spectrum was at 8 cm^{-1} resolution and 64 scans were obtained. The obtained spectra of the suspected particles were compared with the database on the instrument. If the matching rate exceeds 75%, the particles can be confirmed as corresponding microplastics.

Utmost precautions were taken to prevent possible artificial contamination. All the sampling tools were washed thoroughly with Milli-Q water prior to use in the field. The sediment samples were transported and stored in non-plastic containers. All stages of sample processing, extraction, and identification were performed under a clean laminar flow cabinet in an ultra-clean laboratory. Unless stated otherwise, the material of all laboratory wares was non-plastic (glass or stainless steel). Prior to use, all the glassware (e.g. beakers, filtration system, glass filters and glass dishes) were carefully rinsed with Milli-Q water and heated at 450 °C for 4 h to remove any organic material. Nitrile gloves and cotton lab coats were worn during all laboratory activities. Aluminium foil and glass dish covers were applied to all wares and samples to prevent contamination. Milli-Q water and air were drawn through the clean filter to determine the potential airborne plastic contamination. The procedure blanks were also prepared in triplicate. The procedural blank controls were then subjected to microplastic identification to determine background contamination. No microplastic particles were identified in any blank samples.

Mass conversion. The mass of individual plastic particles was calculated by multiplying morphology-specific volumes with the empirical density coefficient. Particle volume was estimated based on particle morphology and dimensions (length), which were recorded according to FTIR images. For fragments and films, the particle volume was calculated as $V_1 = L^3 \times \alpha$, in which α is a shape factor ($\alpha = 0.1$)[75]. For fibres, the particle volume was derived as $V_2 = \pi r^2 \times L$[76]. We used an average microplastic density of 0.98 g cm^{-3}[77]. The calculated equations were as follows:

$$W_{film, ffragment} = \rho \times V_1 = \rho \times L^3 \times \alpha \qquad (1)$$

$$W_{fibre} = \rho \times V_2 = \rho \times \pi r^2 \times L \qquad (2)$$

$$M_{microplastic} = \frac{\sum_1^n M_{film} + \sum_1^m M_{fragment} + \sum_1^j M_{fibre}}{n + m + j} \qquad (3)$$

where W represents the mass of an individual particle; M refers to the average mass of a microplastic particle; ρ is the average density of microplastics, 0.98 g cm^{-3}[77]; L

is the length of microplastics and measured on the stereo microscope, μm; r is the radius of the fibre microplastics and assumed to be 10 μm (the median radius of fibres)[76]; and n, m and j are the numbers of fibres, films and fragments, respectively.

Estimating the load of sedimentary microplastics. The quantitative and mass loads of microplastics were calculated using the estimates of the annual siltation volume from the *Yangtze River Sediment Bulletin*, which was published by the *Changjiang Water Resources Commission of the Ministry of Water Resources*[62,77]. Due to the application of the dam's operating mode of storing clear water and discharging muddy water, as well as the construction of the upstream cascade reservoirs, the sediment budget in the reservoir bed has kept decreasing. Sediment deposition in the TGR was 185.6, 27.8, 59.1 and 144.3 million tons in 2008, 2015, 2019 and 2020, respectively[62,73]. The annual quantitative microplastic load was estimated by multiplying their particle concentrations by the annual sediment deposition. The mass budget was calculated by multiplying the microplastic concentration by the accumulated sediment amount and the average particle mass was calculated via mass conversion.

Mapping and ranking global microplastic contamination in freshwater sediments. In order to compare the microplastic contamination in this study with a global dataset, a global inventory of microplastic contamination in freshwater sediments was collected and listed in Supplementary Table 3. The reported articles were searched through the Web of Science, and the keywords were 'microplastics' and 'sediments'. Different units have been used to describe the sedimentary microplastic concentrations, which enhances complexity when comparing the values in the literature. Thus, from the retrieved literature, only studies with consistent or convertible units (items kg^{-1}) were screened and mapped in Fig. 4. Since no standardised sampling and analysis methods have been established, the size range of the focused microplastics was not well constrained. Detailed information on the particle size distribution of identified microplastics, the extraction methodologies, and the identification techniques were provided in Supplementary Table 3.

Statistical analysis. Statistical analyses were performed using SPSS (SPSS Inc., Chicago, USA). The statistical comparison of microplastic abundance in the upstream and downstream regions and different reaches in 2020, as well as that in different sampling years, was based on the independent samples t-test. The global dataset collected via the Web of Science was mapped using ArcGIS 10.2. Other figures were drawn using OriginPro 2021. Significant differences were assessed at the level of 0.05 and 0.01. All values were reported as mean ± standard deviation (SD).

Reporting summary. Further information on research design is available in the Nature Portfolio Reporting Summary linked to this article.

Data availability

References
1. Pabortsava, K. & Lampitt, R. S. High concentrations of plastic hidden beneath the surface of the Atlantic Ocean. *Nat. Commun.* **11**, 4073 (2020).
2. Peeken, I. et al. Arctic sea ice is an important temporal sink and means of transport for microplastic. *Nat. Commun.* **9**, 1505 (2018).
3. Trainic, M. et al. Airborne microplastic particles detected in the remote marine atmosphere. *Commun. Earth Environ.* **1**, 64 (2020).
4. Napper, I. E. et al. Reaching new heights in plastic pollution—preliminary findings of microplastics on Mount Everest. *One Earth* **3**, 621–630 (2020).
5. Pohl, F., Eggenhuisen, J. T., Kane, I. A. & Clare, M. A. Transport and burial of microplastics in deep-marine sediments by turbidity currents. *Environ. Sci. Technol.* **54**, 4180–4189 (2020).
6. Eriksen, M. et al. Plastic pollution in the World's Oceans: more than 5 trillion plastic pieces weighing over 250,000 tons afloat at sea. *PLoS ONE* **9**, e111913 (2014).
7. van Sebille, E. et al. A global inventory of small floating plastic debris. *Environ. Res. Lett.* **10**, 124006 (2015).
8. Lebreton, L. C. M. et al. River plastic emissions to the world's oceans. *Nat. Commun.* **8**, 15611 (2017).
9. Jambeck, J. R. et al. Plastic waste inputs from land into the ocean. *Science* **347**, 768–771 (2015).
10. Mai, L. et al. Global riverine plastic outflows. *Environ. Sci. Technol.* **54**, 10049–10056 (2020).
11. Andrady, A. L. Microplastics in the marine environment. *Mar. Pollut. Bull.* **62**, 1596–1605 (2011).
12. Hurley, R., Woodward, J. & Rothwell, J. J. Microplastic contamination of river beds significantly reduced by catchment-wide flooding. *Nat. Geosci.* **11**, 251–257 (2018).
13. Nilsson, C., Reidy, C. A., Dynesius, M. & Revenga, C. Fragmentation and flow regulation of the world's large river systems. *Science* **308**, 405 (2005).
14. Belletti, B. et al. More than one million barriers fragment Europe's rivers. *Nature* **588**, 436–441 (2020).
15. Liu, M. et al. Sources and transport of methylmercury in the Yangtze River and the impact of the Three Gorges Dam. *Water Res.* **166**, 115042 (2019).
16. Watkins, L., McGrattan, S., Sullivan, P. J. & Walter, M. T. The effect of dams on river transport of microplastic pollution. *Sci. Total Environ.* **664**, 834–840 (2019).
17. Zhang, K., Gong, W., Lv, J., Xiong, X. & Wu, C. Accumulation of floating microplastics behind the Three Gorges Dam. *Environ. Pollut.* **204**, 117–123 (2015).
18. Martin, C. et al. Exponential increase of plastic burial in mangrove sediments as a major plastic sink. *Sci. Adv.* **6**, eaaz5593 (2020).
19. Di, M. & Wang, J. Microplastics in surface waters and sediments of the Three Gorges Reservoir, China. *Sci. Total Environ.* **616–617**, 1620–1627 (2018).
20. Nthunya, L. N., Khumalo, N. P., Verliefde, A. R., Mamba, B. B. & Mhlanga, S. D. Quantitative analysis of phenols and PAHs in the Nandoni Dam in Limpopo Province, South Africa: a preliminary study for dam water quality management. *Phys. Chem. Earth Parts A/B/C* **112**, 228–236 (2019).
21. Maavara, T. et al. River dam impacts on biogeochemical cycling. *Nat. Rev. Earth Environ.* **1**, 103–116 (2020).
22. Xu, D., Gao, B., Wan, X., Peng, W. & Zhang, B. Influence of catastrophic flood on microplastics organization in surface water of the Three Gorges Reservoir, China. *Water Res.* **211**, 118018 (2022).
23. Lin, L. et al. Distribution and source of microplastics in China's second largest reservoir—Danjiangkou Reservoir. *J. Environ. Sci.* **102**, 74–84 (2021).
24. Zhang, K. et al. Occurrence and characteristics of microplastic pollution in Xiangxi Bay of Three Gorges Reservoir, China. *Environ. Sci. Technol.* **51**, 3794–3801 (2017).
25. Guo, Z. et al. Global meta-analysis of microplastic contamination in reservoirs with a novel framework. *Water Res.* **207**, 117828 (2021).
26. Lu, H.-C., Ziajahromi, S., Neale, P. A. & Leusch, F. D. L. A systematic review of freshwater microplastics in water and sediments: recommendations for harmonisation to enhance future study comparisons. *Sci. Total Environ.* **781**, 146693 (2021).
27. Chen, Y., Gao, B., Xu, D., Sun, K. & Li, Y. Catchment-wide flooding significantly altered microplastics organization in the hydro-fluctuation belt of the reservoir. *iScience* **25**, 104401 (2022).
28. Wang, Z. et al. Preferential accumulation of small (<300 μm) microplastics in the sediments of a coastal plain river network in eastern China. *Water Res.* **144**, 393–401 (2018).
29. Cai, M. et al. Lost but can't be neglected: huge quantities of small microplastics hide in the South China Sea. *Sci. Total Environ.* **633**, 1206–1216 (2018).
30. Enders, K., Lenz, R., Beer, S. & Stedmon, C. A. Extraction of microplastic from biota: recommended acidic digestion destroys common plastic polymers. *ICES J. Mar. Sci* **74**, 326–331 (2017).
31. Eo, S. et al. Prevalence of small high-density microplastics in the continental shelf and deep sea waters of East Asia. *Water Res.* **200**, 117238 (2021).
32. Leiser, R. et al. Interaction of cyanobacteria with calcium facilitates the sedimentation of microplastics in a eutrophic reservoir. *Water Res.* **189**, 116582 (2021).
33. Feng, S. et al. Microplastic footprints in the Qinghai-Tibet Plateau and their implications to the Yangtze River Basin. *J. Hazard. Mater.* **407**, 124776 (2021).
34. Zhao, S. et al. Analysis of suspended microplastics in the Changjiang Estuary: implications for riverine plastic load to the ocean. *Water Res.* **161**, 560–569 (2019).
35. Veerasingam, S., Mugilarasan, M., Venkatachalapathy, R. & Vethamony, P. Influence of 2015 flood on the distribution and occurrence of microplastic pellets along the Chennai coast, India. *Mar. Pollut. Bull.* **109**, 196–204 (2016).
36. Lee, J. et al. Relationships among the abundances of plastic debris in different size classes on beaches in South Korea. *Mar. Pollut. Bull.* **77**, 349–354 (2013).
37. Lattin, G. L., Moore, C. J., Zellers, A. F., Moore, S. L. & Weisberg, S. B. A comparison of neustonic plastic and zooplankton at different depths near the southern California shore. *Mar. Pollut. Bull.* **49**, 291–294 (2004).
38. Moore, C. J., Moore, S. L., Weisberg, S. B., Lattin, G. L. & Zellers, A. F. A comparison of neustonic plastic and zooplankton abundance in southern California's coastal waters. *Mar. Pollut. Bull.* **44**, 1035–1038 (2002).
39. Zhang, K. et al. The hydro-fluctuation belt of the Three Gorges Reservoir: source or sink of microplastics in the water? *Environ. Pollut.* **248**, 279–285 (2019).
40. Leiser, R., Wu, G.-M., Neu, T. R. & Wendt-Potthoff, K. Biofouling, metal sorption and aggregation are related to sinking of microplastics in a stratified reservoir. *Water Res.* **176**, 115748 (2020).

41. Lobelle, D. et al. Global modeled sinking characteristics of biofouled microplastic. *J. Geophys. Res. Oceans* **126**, e2020JC017098 (2021).
42. Miao, L. et al. Effects of biofilm colonization on the sinking of microplastics in three freshwater environments. *J. Hazard. Mater.* **413**, 125370 (2021).
43. Li, Y. et al. Interactions between nano/micro plastics and suspended sediment in water: Implications on aggregation and settling. *Water Res.* **161**, 486–495 (2019).
44. Xu, Y. et al. Influence of dissolved black carbon on the aggregation and deposition of polystyrene nanoplastics: Comparison with dissolved humic acid. *Water Res.* **196**, 117054 (2021).
45. Junaid, M. & Wang, J. Interaction of nanoplastics with extracellular polymeric substances (EPS) in the aquatic environment: a special reference to eco-corona formation and associated impacts. *Water Res.* **201**, 117319 (2021).
46. Zhao, S., Ward, J. E., Danley, M. & Mincer, T. J. Field-based evidence for microplastic in marine aggregates and mussels: implications for trophic transfer. *Environ. Sci. Technol.* **52**, 11038–11048 (2018).
47. Ye, S. & Andrady, A. L. Fouling of floating plastic debris under Biscayne Bay exposure conditions. *Mar. Pollut. Bull.* **22**, 608–613 (1991).
48. Poulain, M. et al. Small microplastics as a main contributor to plastic mass balance in the North Atlantic Subtropical Gyre. *Environ. Sci. Technol.* **53**, 1157–1164 (2019).
49. Amaral-Zettler, L. A., Zettler, E. R., Mincer, T. J., Klaassen, M. A. & Gallager, S. M. Biofouling impacts on polyethylene density and sinking in coastal waters: a macro/micro tipping point? *Water Res.* **201**, 117289 (2021).
50. Chen, X., Xiong, X., Jiang, X., Shi, H. & Wu, C. Sinking of floating plastic debris caused by biofilm development in a freshwater lake. *Chemosphere* **222**, 856–864 (2019).
51. Enders, K., Lenz, R., Stedmon, C. A. & Nielsen, T. G. Abundance, size and polymer composition of marine microplastics ≥10μm in the Atlantic Ocean and their modelled vertical distribution. *Mar. Pollut. Bull.* **100**, 70–81 (2015).
52. Kooi, M. et al. The effect of particle properties on the depth profile of buoyant plastics in the ocean. *Sci. Rep.* **6**, 33882 (2016).
53. Reisser, J. et al. The vertical distribution of buoyant plastics at sea: an observational study in the North Atlantic Gyre. *Biogeosciences* **12**, 1249–1256 (2015).
54. Fazey, F. M. C. & Ryan, P. G. Biofouling on buoyant marine plastics: an experimental study into the effect of size on surface longevity. *Environ. Pollut.* **210**, 354–360 (2016).
55. Yao, P. et al. A review of microplastics in sediments: spatial and temporal occurrences, biological effects, and analytic methods. *Quat. Int.* **519**, 274–281 (2019).
56. Niu, J., Gao, B., Wu, W., Peng, W. & Xu, D. Occurrence, stability and source identification of small size microplastics in the Jiayan reservoir, China. *Sci. Total Environ.* **807**, 150832 (2022).
57. Jiménez-Skrzypek, G. et al. Microplastic-adsorbed organic contaminants: analytical methods and occurrence. *Trends Analyt. Chem.* **136**, 116186 (2021).
58. Zumstein, M. T. et al. Biodegradation of synthetic polymers in soils: tracking carbon into CO_2 and microbial biomass. *Sci. Adv.* **4**, eaas9024 (2018).
59. Chen, Y. et al. Tracking microplastics biodegradation through CO2 emission: role of photoaging and mineral addition. *J. Hazard. Mater.* **439**, 129615 (2022).
60. Lee, Y. K., Murphy, K. R. & Hur, J. Fluorescence signatures of dissolved organic matter leached from microplastics: polymers and additives. *Environ. Sci. Technol.* **54**, 11905–11914 (2020).
61. Zhang, E. et al. The photo-redox of chromium regulated by microplastics (MPs) and MPs-derived dissolved organic matter (MPs-DOM) and the CO2 emission of MPs-DOM. *Fundam. Res.* https://doi.org/10.1016/j.fmre.2022.08.009 (2022).
62. Changjiang Water Resources Commission of the Ministry of Water Resources. *Yangtze River Sediment Bulletin*. http://www.cjw.gov.cn/ (2008−2020).
63. PlasticEurope. Plastics—The Facts 2020, An analysis of European plastics production, demand and waste data. 1-42 (2020).
64. Weiss, L. et al. The missing ocean plastic sink: gone with the rivers. *Science* **373**, 107–111 (2021).
65. He, K. et al. Effects of cascade dams on the occurrence and distribution of microplastics in surface sediments of Wujiang river basin, Southwestern China. *Ecotoxicol. Environ. Saf.* **240**, 113715 (2022).
66. Dhivert, E., Phuong, N. N., Mourier, B., Grosbois, C. & Gasperi, J. Microplastic trapping in dam reservoirs driven by complex hydrosedimentary processes (Villerest Reservoir, Loire River, France). *Water Res.* **225**, 119187 (2022).
67. Hidalgo-Ruz, V., Gutow, L., Thompson, R. C. & Thiel, M. Microplastics in the marine environment: a review of the methods used for identification and quantification. *Environ. Sci. Technol.* **46**, 3060–3075 (2012).
68. Rocha-Santos, T. & Duarte, A. C. A critical overview of the analytical approaches to the occurrence, the fate and the behavior of microplastics in the environment. *Trends Anal. Chem.* **65**, 47–53 (2015).
69. Dams, I. C. O. L. *World Register of Dams: Database Presentation* 2020).
70. Yang, Y. et al. Influence of large reservoir operation on water-levels and flows in reaches below dam: case study of the Three Gorges Reservoir. *Sci. Rep.* **7**, 15640 (2017).
71. Ren, S., Zhang, B., Wang, W.-J., Yuan, Y. & Guo, C. Sedimentation and its response to management strategies of the Three Gorges Reservoir, Yangtze River, China. *CATENA* **199**, 105096 (2021).
72. Ren, J. et al. Impact of the construction of cascade reservoirs on suspended sediment peak transport variation during flood events in the Three Gorges Reservoir. *CATENA* **188**, 104409 (2020).
73. Masura, J., Baker, J., Foster, G. & Arthur, C. Laboratory methods for the analysis of microplastics in the marine environment: recommendations for quantifying synthetic particles in waters and sediments. *NOAA Technical Memorandum NOS-OR&R-48* (2015).
74. Masura, J., Baker, J. E., Foster, G. D., Arthur, C. & Herring, C. Laboratory methods for the analysis of microplastics in the marine environment: recommendations for quantifying synthetic particles in waters and sediments. (2015).
75. Cózar, A. et al. Plastic debris in the open ocean. *Proc. Natl Acad. Sci.* **111**, 10239 (2014).
76. Jung, J.-W. et al. Ecological risk assessment of microplastics in coastal, shelf, and deep sea waters with a consideration of environmentally relevant size and shape. *Environ. Pollut.* **270**, 116217 (2021).
77. Senathirajah, K. et al. Estimation of the mass of microplastics ingested—A pivotal first step towards human health risk assessment. *J. Hazard. Mater.* **404**, 124004 (2021).

Acknowledgements

Author contributions

B.G. acquired financial support and initiated the microplastics project. B.G. and Y.C. designed the study, conducted the analyses and co-authored the manuscript. D.X. undertook the field sampling, provided the analytical guidance and contributed to the manuscript. K.S. and B.X. assisted in the preparation and revision of the manuscript.

Competing interests

The authors declare no competing interests.

Additional information

Supplementary information The online version contains supplementary material available at https://doi.org/10.1038/s43247-023-00701-z.

Correspondence and requests for materials should be addressed to Bo Gao.

Peer review information *Communications Earth & Environment* thanks Jingfu Wang and the other, anonymous, reviewer(s) for their contribution to the peer review of this work. Primary Handling Editors: Clare Davis.

Reprints and permission information is available at http://www.nature.com/reprints

Publisher's note Springer Nature remains neutral with regard to jurisdictional claims in published maps and institutional affiliations.